Magnetic coupling of single Co adatoms to a Co underlayer through a Pd spacer of variable thickness

L. V. Dzemiantsova,* M. Hortamani, C. Hanneken, A. Kubetzka, K. von Bergmann, and R. Wiesendanger
Institute of Applied Physics, University of Hamburg, Jungiusstrasse 11, D-20355 Hamburg, Germany
(Received 3 August 2012; published 21 September 2012)

We have performed a combined experimental and theoretical investigation of Co atoms on top of a Pd spacer on Co/Ir(111). Using spin-polarized scanning tunneling microscopy and spectroscopy we first studied the morphology and the spin-resolved electronic properties of mono- and double-layer Pd on Co/Ir(111). We find pseudomorphic growth with two stackings of the Pd monolayer, which can easily be distinguished electronically by measuring the differential tunneling conductance. Spin contrast is achieved on both the Pd mono- and double-layer and on Co adatoms on top, which means that the electron density above the surfaces and adatoms is spin-polarized. Indeed, based on our *ab initio* calculations, we find that the surface Pd atoms of mono- and double-layer carry an induced magnetic moment of about 0.3 and 0.2 μ_B, respectively; Co layers adsorbed on top of a Pd mono- and double-layer possess a magnetic moment of about 2.0 μ_B/atom. In accordance with our experimental observations of Co atoms on the Pd spacer, the calculations also show that Co adlayers are ferromagnetically coupled to the Co/Ir(111) underneath. The size of the magnetic exchange coupling is reduced by a factor of three from a mono- to double-layer Pd spacer between the Co layers.

DOI: 10.1103/PhysRevB.86.094427 PACS number(s): 07.79.Cz, 71.15.Mb, 68.37.Ef

I. INTRODUCTION

Magnetic atoms adsorbed on nonmagnetic surfaces have become an active research topic in the past few years due to their importance in the fundamental understanding of magnetism and practical applications for spin-based computing schemes.[1] In particular, knowledge about the magnetic interactions on the atomic scale is crucial for tailoring magnetic devices in reduced dimensions and tuning their properties.[2]

In this study, we design a system consisting of individual magnetic atoms adsorbed on a layer of nonmagnetic material, a spacer layer, grown on a magnetic monolayer (ML) on a substrate in order to investigate the magnetic properties of the adatoms, and their evolution with increasing spacer layer thickness. Motivated by theoretical investigations,[3] the dependence of the exchange coupling of magnetic adatoms on the thickness of the spacer layer is in the focus of our current investigation.

We have chosen individual Co atoms and a Co monolayer (ML) on Ir(111) as magnetic units. In general, the spacer can be metallic or nonmetallic. In previous work with metallic overlayers on magnetic systems it has been reported that spin contrast of Fe/W(110) and Fe/Mo(110) can penetrate through thin Pb films[4] and small Au clusters,[5] respectively. Magnetic domain structures of substrates have also been observed when they were covered with a nonmetallic spacer; i.e., the magnetic pattern of Ni(111) and Co/Ir(111) was observed through one atomic layer of carbon.[6,7] It was also shown that a magnetic vortex structure of Fe/W(110) can be probed through a sulfur overlayer.[8] However, self-terminated monolayer growth of the nonmetallic materials,[6,8] a quantum size effect of Pb structures,[4,9] and AuFe alloy formation[5] make these systems complicated for the current research focus on the magnetic coupling of single atoms through spacer layers of different thickness. In the present work we have decided to use Pd as a metallic spacer material. Indeed, Pd possesses very intriguing properties: As bulk it is paramagnetic but its density of states, which is strongly enhanced at the Fermi level E_F, only barely fails to satisfy the Stoner criterion[10]; Pd films get easily polarized in the vicinity of Fe or Co.[11]

The system of $CoPd_nCo/Ir(111)$ was examined by means of spin-polarized scanning tunneling microscopy (SP-STM) and spectroscopy (SP-STS).[12] Using this technique it is possible to resolve the electronic and magnetic structure on an atomic scale. For a deeper understanding of the observations made in our SP-STM experiments, we performed spin-resolved density functional theory (DFT) calculations. This paper is organized as follows: In Sec. II we provide details on the experimental method and sample preparation as well as the calculations for the system studied. In Sec. III we first show the results on the Pd adlayers and then turn to the findings for Co atoms adsorbed on top. In Sec. IV all results of the system studied are summarized.

II. EXPERIMENTAL AND THEORY DETAILS

A. Experimental details

Our experiments were carried out in a home-built STM at $T = 8.0 \pm 0.5$ K in ultrahigh vacuum.[13] After cleaning the Ir(111) single crystal by repeated cycles of Ar^+-sputtering and annealing to $T = 1300$ K for 1 min, Co was subsequently deposited at a rate of about 1 ML/min. After cooling the Co/Ir(111) sample for 30–60 min, Pd was evaporated at a rate of about 0.05 ML/min from a 1-mm palladium rod heated by electron bombardment. Co atoms were deposited onto the cold sample inside the STM ($T_{max} = 20$ K) to prevent diffusion. The magnetic tips were prepared by coating flashed W tips ($T \approx 2000$ K) with 45 ML of Fe followed by annealing at $T \approx 500$ K for 5 min. Constant-current (I) images (topography) and maps of differential tunneling conductance (dI/dU)[14,15] were measured simultaneously with closed feedback loop using lock-in technique by adding a modulation voltage U_{mod} to the sample bias U. Single dI/dU spectra were taken at specific positions with the tip-sample distance stabilized at U_{stab} and I_{stab} before switching off the feedback loop.

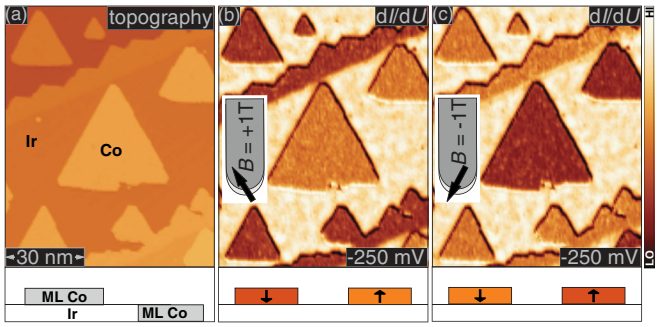

FIG. 1. (Color online) SP-STM measurements of Co/Ir(111) with an Fe-coated W tip: (a) Constant current image measured at $B = +1$ T. (b) and (c) Spin-polarized dI/dU maps measured at $B = +1$ T and $B = -1$ T, respectively. Color bar shows variations of the spin-polarized dI/dU signal. Sketches in (b) and (c) schematically illustrate the principle of inversion of the magnetic out-of-plane contrast. Measurement parameters: $I = 2$ nA, $U = -250$ mV, and $U_{\mathrm{mod}} = 20$ mV.

Figure 1 shows a sample of Co/Ir(111) where Co forms pseudomorphic single-stacking single-domain ferromagnetic islands with out-of-plane magnetic anisotropy.[16] A magnetic field of $B = \pm 1$ T was used to align the Fe-coated W tip's magnetization such that it possesses a significant out-of-plane component, whereas the magnetization of Co/Ir(111) stays unaffected [see Figs. 1(b, c)].[16] We found that this is also the case for Pd-covered Co/Ir(111) and therefore we will make use of the possibility to align the tip magnetization in an external magnetic field ($1\ \mathrm{T} \leqslant |B| \leqslant 2\ \mathrm{T}$) throughout this study.

B. Theory details

Our theoretical study has been performed by first-principles calculations based on DFT. We employed the full-potential linearized augmented plane wave method in film mode as implemented in the FLEUR code.[17] We have applied the generalized gradient approximation of Perdew, Burke, and Ernzerhof. We modeled the system with a slab containing 7 layers of Ir with in-plane lattice constant 2.75 Å (corresponding to the calculated fcc lattice constant of $a_0 = 3.89$ Å) and equivalent layers on each side of the slab. The systems were relaxed including the two topmost layers of the Ir substrate in the direction of the surface normal until the atomic forces were smaller than 3×10^{-5} hrt/a.u.. We chose muffin-tin radii of 2.4 a.u. for both Ir and Pd and 2.3 a.u. for Co atoms. Self-consistency of the calculation is reached by setting the plane wave cut-off for the basis function to $k_{\mathrm{max}} = 3.8$ a.u.$^{-1}$ and 72 $k_{\parallel}$ points in the irreducible Brillouin zone. The exchange energy of a system, E_{exc}, is calculated as the difference between the total energies of fully self-consistent ferromagnetic (FM) and antiferromagnetic (AFM) configurations.

We considered closed pseudomorphic layers of Co/Ir(111), Pd_nCo/Ir(111) (n = 1–2), and CoPd_nCo/Ir(111) (n = 1–3) with different stackings. We found that fcc Co is energetically favored over hcp by amount of 25 meV/atom, in agreement with the experimental observation of only one type of stacking of Co (cf. Fig. 1). A calculation of a row-wise AFM Co/Ir(111) layer covered with a ML Pd (both stackings fcc) yields an increase in energy of $E = 167$ meV/Co atom compared to the FM state. For CoPdCo/Ir(111) we also calculated a (2×2) Co atom superstructure on top of PdCo/Ir(111) in addition to the fully closed Co ML on PdCo/Ir(111). A larger Pd spacer thickness was not considered for the calculations due to the tremendous increase in computation time.

III. RESULTS

A. Pd adlayers on Co/Ir(111)

1. Experiment

A typical constant-current image of the sample of 1 ML Pd on Co/Ir(111) is shown in Fig. 2(a), where four buried monoatomic steps of the Ir(111) surface can be observed. The deposited Co forms ML high triangular islands on the Ir terraces and ML high wires attached to the Ir(111) step edges.[16] In the submonolayer regime, Pd of ML height grows on top of Co and decorates Co rims [see the sketch of Fig. 2(a)]. A small amount of ML Pd can be found on the Co-free area of the bare Ir(111), too. In this coverage regime the growth of both Co and Pd is pseudomorphic with no sign of intermixing. We observe a fractal growth of Pd with a randomly branched structure with no preferential orientation.[19,20] We find that the fractal fine structure varies with the experimental conditions such as the deposition rate, the amount of deposited material, and temperature of the substrate, similar to the reports for the fractal pattern formation of Ag/Pt(111),[20] Pt/Pt(111),[21,22] Au/Ru(0001),[23] and Ag/Pt(111)[19,20] and theoretical predictions.[24]

Figure 2(b) shows a constant-current image of the same region as Fig. 2(a) colorized with the simultaneously acquired dI/dU signal at $U = +100$ mV; to simplify the discussion at this point we chose an image taken at a bias voltage where the spin-polarized contribution to the signal vanishes for both Co as well as Pd on Co layers. In agreement with previous results[16] we observe a single dI/dU level on all Co ML areas, due to the preferred growth with only one type of stacking. In contrast, for PdCo two different contrast levels are observed, which we interpret as the two possible stackings of the Pd monolayer on Co/Ir(111), labeled Pd_A and Pd_B in the following.

Next, we show the sample measured at a bias voltage such that both stacking and magnetic contrasts are observed. Figure 2(c) displays the constant-current image colorized with the dI/dU signal at $U = -400$ mV, for which the magnetism of Co is detected as well. In the following, Co islands presenting the higher dI/dU signal at $U = -400$ mV are referred to as Co↑, while Co islands with the lower dI/dU signal are denoted by Co↓ (for tip magnetization along $+B$). This notation is arbitrary since the relative orientation of tip and island magnetization is unknown. A significant contrast is also visible on PdCo, which has its origin in a different stacking as well as different magnetization directions. The two contributions can be disentangled by either comparing with the non-spin-polarized dI/dU map of Fig. 2(b) or comparing with a dI/dU map with opposite z-magnetization component of the tip [Fig. 2(d)]. For the latter case, the magnetic contributions to the contrast are inverted. The observation of spin contrast on Pd means that the local density of states (LDOS) measured a few angstroms above the surface is substantially spin-polarized. By

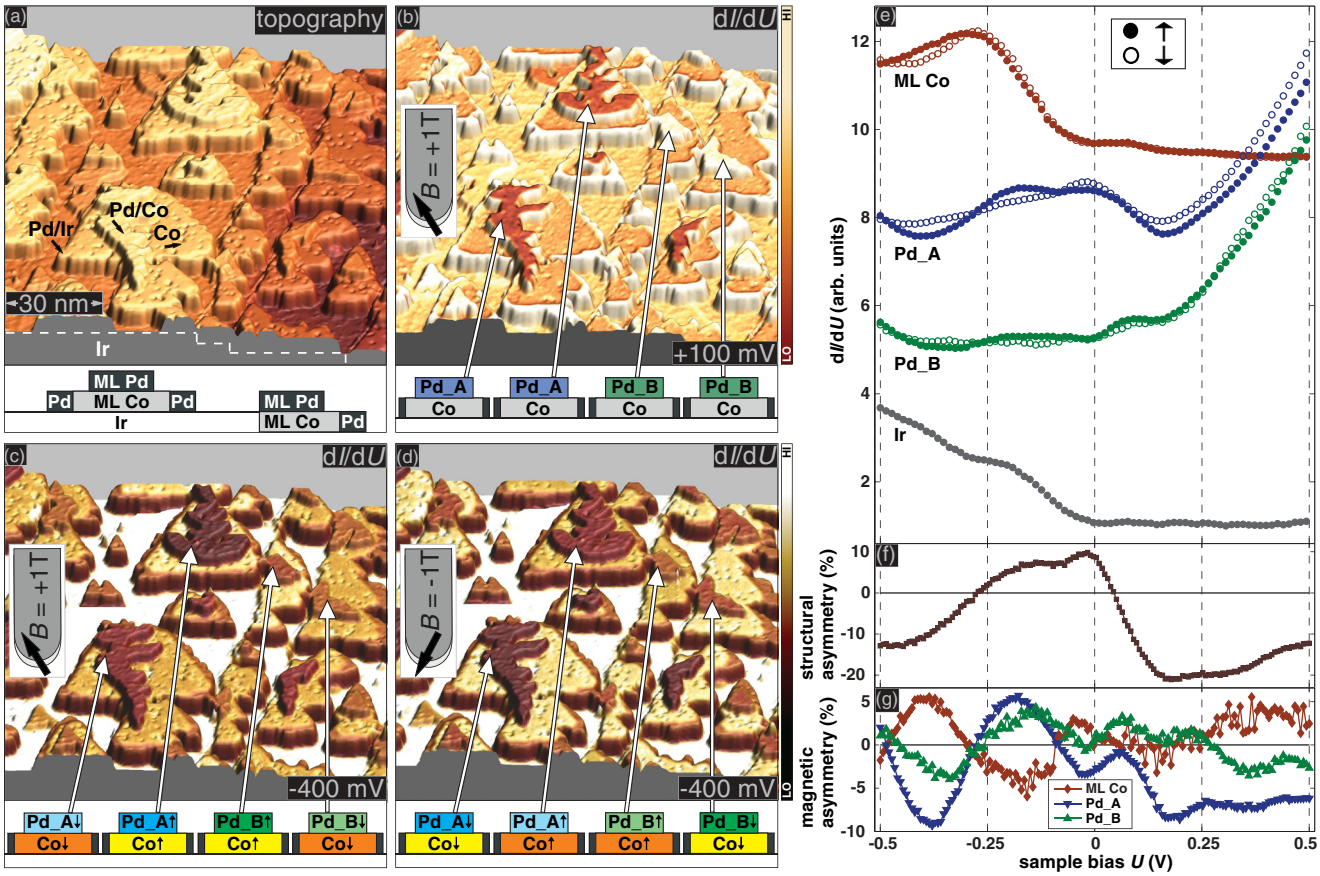

FIG. 2. (Color online) SP-STM measurements of ML Pd on Co/Ir(111): (a) Constant-current image and (b) Constant-current image colorized with the simultaneously acquired dI/dU signal at $U = +100$ mV where the spin-polarized contribution vanishes, measured at $B = +1$ T. (b) and (c) Constant-current images of the same sample area colorized with the simultaneously acquired spin-resolved dI/dU signal at $U = -400$ mV, measured at $B = +1$ T and $B = -1$ T, respectively. Color bars show variations of the spin-polarized dI/dU signal. Sketches schematically demonstrate contrast levels observed on Co and PdCo. Measurement parameters: $I = 0.8$ nA and $U_{\text{mod}} = 25$ mV. (e) Spin-resolved dI/dU spectra ($U_{\text{stab}} = -500$ mV, $I_{\text{stab}} = 0.8$ nA, $U_{\text{mod}} = 25$ mV) measured at $B = +1$ T. Each spectrum displayed is an average of five single spectra. Co and PdCo spectra are shifted vertically by multiples of 3 arb. units for clarity. (f) Structural asymmetry calculated for spin-averaged spectra[18] of PdCo of different stacking, namely Pd_A and Pd_B. (g) Magnetic asymmetries calculated for spin-resolved spectra of ML Co, Pd_A, and Pd_B.

comparison to Fig. 2(b), we denote Pd films of one stacking as Pd_A↑ (Pd_B↑) if residing on Co↑ islands and Pd_A↓ (Pd_B↓) if residing on Co↓ islands. All contrast levels of the sample are schematically shown in the sketches of Figs. 2(c) and 2(d).[25]

To get access to the spin- and energy-resolved electronic structure of the surface, we performed SP-STS. Figure 2(e) shows the spin-resolved dI/dU spectra obtained above Ir(111), ML Co↑,↓, Pd_A↑,↓, and Pd_B↑,↓, at $B = +1$ T. The Ir(111) spectrum exhibits an increasing dI/dU signal toward more negative bias below E_{F}, and the spin-polarized dI/dU spectra of ML Co are rather featureless in the positive bias regime but have a characteristic peak at $U \approx -270$ mV, in good qualitative agreement with the previous study in Ref. 16. We observe that all spectra of PdCo exhibit an increasing dI/dU signal above E_{F} and no outstanding spectroscopic features below E_{F}.

To distinguish the spectroscopic differences due to stacking from those due to magnetism, we calculate the structural and the magnetic asymmetry of the spectra. The asymmetry is defined by

$$A(U) = \frac{dI/dU(U)_1 - dI/dU(U)_2}{dI/dU(U)_1 + dI/dU(U)_2}. \quad (1)$$

For the structural asymmetry we use dI/dU_{A} and dI/dU_{B} which are the calculated spin-averaged spectra[18] of Pd_A and Pd_B, respectively; for the magnetic asymmetry we use $dI/dU_{\uparrow}$ and $dI/dU_{\downarrow}$ which are the spin-resolved spectra of Co↑ (Pd_A↑, Pd_B↑) and Co↓ (Pd_A↓, Pd_B↓), respectively. The structural asymmetry is plotted in Fig. 2(f) and shows that the two different stackings can be distinguished easily in the whole bias regime studied. The magnetic asymmetries of ML Co, Pd_A and Pd_B are shown in Fig. 2(g). Interestingly, asymmetries of Pd_A and Pd_B go mostly parallel in the negative bias regime and have the opposite sign compared to that of ML Co. All magnetic asymmetries are in the same range of values up to 5–10 %.

To investigate whether we can still achieve a spin-polarized signal for a double-layer (DL) of Pd on Co/Ir(111), i.e., Pd_2Co, we prepared a sample as shown in Fig. 3(a). In this image,

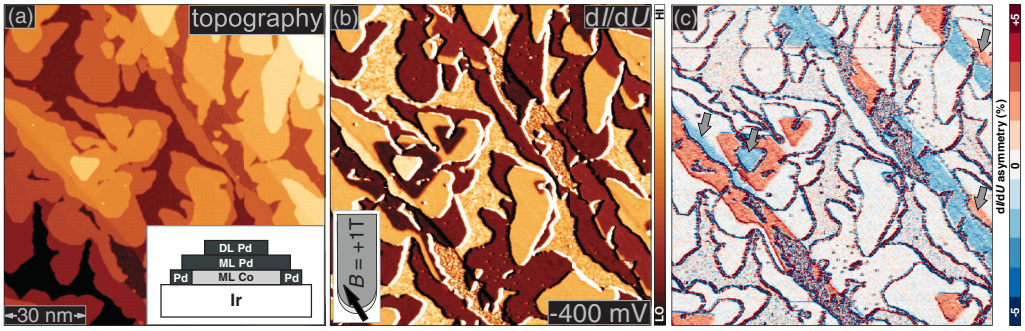

FIG. 3. (Color online) SP-STM measurements of a sample exhibiting ML Pd as well as DL Pd on Co/Ir(111): (a) Constant-current image and (b) simultaneously acquired spin-resolved dI/dU map measured at $B = +1$ T. Color bar shows variations of the spin-polarized dI/dU signal. (c) Spatially resolved magnetic asymmetry map derived from spin-resolved dI/dU maps taken at magnetic field values of $B = \pm 1$ T; DL Pd areas are indicated by gray arrows. Measurement parameters: $I = 1$ nA, $U = -400$ mV, and $U_{\text{mod}} = 30$ mV.

three buried monoatomic steps of the Ir(111) substrate can be observed. The inset of Fig. 3(a) schematically illustrates the surface studied: while ML Pd covers and decorates ML Co, nucleation of DL Pd on top of it also occurs. Figure 3(b) shows a spin-resolved dI/dU map of the same sample area; again stacking- as well as magnetism-dependent contributions account for the dI/dU signal. To extract the magnetic contributions only, again a field inversion measurement is performed. Figure 3(c) displays a spatially resolved magnetic asymmetry map obtained by measuring dI/dU maps at $U = -400$ mV and at magnetic fields of $B_{\uparrow} = +1$ T [Fig. 3(b)] and $B_{\downarrow} = -1$ T and using Eq. (1). In such an asymmetry map, areas that are colored exhibit magnetic contrast while those that appear white are nonmagnetic. Here, both PdCo and Pd_2Co areas are colored (for the latter, cf. gray arrows), which means that the LDOS in the vacuum is spin-polarized not only above the ML Pd, but also above the DL Pd. It should be noted that the absolute size of the asymmetry is similar for both ML and DL Pd, even though possibly different stackings are involved; the sign of the asymmetry is determined by the magnetization direction of the sample, i.e., if it is parallel or antiparallel to the tip magnetization at $B = +1$T.

The nature of the spin contrast achieved on ML Pd and DL Pd in Figs. 2(c), 2(d), and 3(b) can in general be of two different origins: Pd is magnetic since it gets polarized by the underlying Co layer, or Pd is nonmagnetic but the magnetism of the Co layer underneath the Pd is probed. While experimentally it is difficult to distinguish between the two effects, the DFT calculations in the next section will clarify the origin.

2. *Theory and discussion*

In SP-STM experiments we observed that ML Pd grows in two stackings on Co/Ir(111) [see Fig. 2(b)]. Indeed, our DFT calculations show that fcc and hcp stackings of PdCo/Ir(111) are coexisting ($E_{\text{fcc}} - E_{\text{hcp}} \approx 2$ meV/atom) on energetically more favorable fcc stacking of Co/Ir(111). From the experiments of the different spin-polarized contrast levels between PdCo (Pd_2Co) islands and the contrast change in magnetic field inversion measurements in Figs. 2(c), 2(d) and 3(b), 3(c), we conclude that Pd-capped Co islands are single domain ferromagnetic with an easy magnetization axis normal to the sample surface. Our DFT calculations confirm that the ground state of PdCo/Ir(111) is FM with magnetic moments of Co and Pd of 1.96 ± 0.03 and 0.31 ± 0.01 μ_B/atom, respectively; the given values are an average of the different possible stacking combinations and the small standard deviation demonstrates that the value is nearly independent of the stacking. In a Pd_2Co/Ir(111) system, the magnetic moments amount to 0.20 for the top Pd layer, 0.37 for the subsurface Pd layer, and 2.05 μ_B/atom for the Co layer (all in fcc stacking); see Fig. 4. These values are in good qualitative agreement with results in Ref. 26, where it was reported that the Co overlayer induces a magnetic moment of 0.33 and 0.24 μ_B in the first and second layer of the Pd substrate, respectively. Our calculations also show that an unsupported Pd layer is nonmagnetic; thus, the magnetic moments of Pd adlayers are induced by the Co layer underneath.

B. Adsorbed Co atoms

1. *Experiment*

After having demonstrated that both the Pd ML and Pd DL are polarized by the underlying Co/Ir(111) system, we study the properties of Co atoms adsorbed on top. A representative topography of Co adatoms on ML Pd on Co/Ir(111) is shown in Fig. 5(a). It exhibits one buried atomic Ir(111) step going from the bottom-left to the upper-right side of the image; a ML Co wire is attached to the Ir step edge and Pd of ML height is grown on top of the Co and decorating Co rims. The individual Co atoms on PdCo are imaged as protrusions of about 2 Å in height.

			↓1% Pd	0.20
		↓6% Pd	0.31 ± 0.01	0.37
↓7%	Co	1.83 ± 0.05	1.96 ± 0.03	2.05
↓0.03%	Ir	0.21 ± 0.03	0.19 ± 0.07	0.19

FIG. 4. Results of DFT calculations of layers of Co/Ir(111) and Pd_nCo/Ir(111) $n = 1$–2: Values inside the layers indicate magnetic moments (μ_B/atom). Values with standard deviations are averages of different stacking combinations. For Pd_2Co/Ir(111) calculations were done for the most stable stacking, namely fcc. The inward relaxations for Pd, Co, and the topmost Ir layer compared to the bulk Ir interlayer distances are shown in percentages.

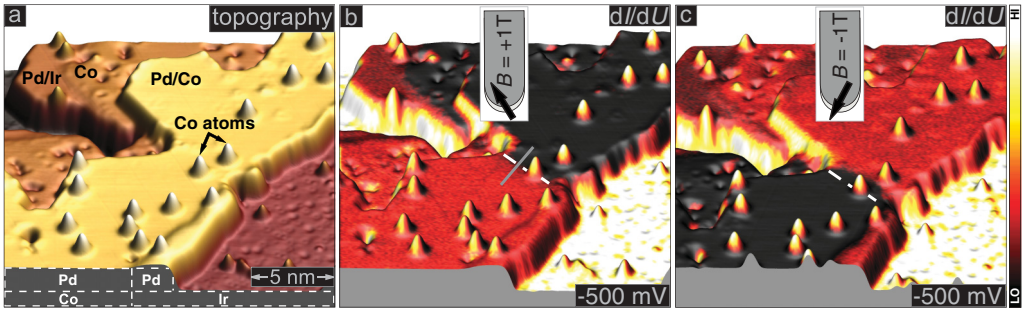

FIG. 5. (Color online) SP-STM measurements of Co atoms on ML Pd on Co/Ir(111): (a) Constant-current image measured at $B = +1$ T. (b) and (c) Constant-current images colorized with the simultaneously acquired spin-resolved dI/dU signal measured at $B = +1$ T and $B = -1$ T, respectively; dashed white line indicates a domain wall being moved upon field reversal. Color bar shows variations of the spin-polarized dI/dU signal. Measurement parameters: $I = 1.5$ nA, $U = -500$ mV, and $U_{\text{mod}} = 30$ mV.

Figure 5(b) displays the topography colorized with the simultaneously acquired dI/dU signal at $U = -500$ mV. In this sample area we find two opposite magnetization directions for Co as well as PdCo, separated by a domain wall (white dashed line) with a width (gray line) of $w = 1.41 \pm 0.11$ nm,[27] which is slightly smaller compared to that found for pure Co/Ir(111) ($w = 2.0 \pm 0.14$ nm).[16] In dI/dU maps at this bias voltage we also observe a different signal intensity for Co adatoms residing on the oppositely magnetized domains of PdCo. Indeed, by inverting the z component of the tip magnetization direction in the external magnetic field, all contrast levels that are of magnetic origin reverse, i.e., Co/Ir(111), PdCo, and Co adatoms on PdCo [Figs. 5(b) and 5(c) measured at $B = +1$ T and $B = -1$ T, respectively). Note that the domain wall has moved by about 1.3 nm within the constriction upon field reversal as seen in Fig. 5(c).

To investigate the spin- and energy-resolved electronic structure of Co atoms, and its evolution with the different spacer thickness, we performed SP-STS measurements of adatoms on ML and DL Pd on Co/Ir(111). Figure 6(a) shows a topography of such a sample. The spectroscopic data measured on this system at $B = \pm 2$ T are shown in Fig. 6(b). The displayed plots are an average over five spectra measured at positions as indicated in Fig. 6(a).

The spectra of ML Pd and DL Pd were recorded on defect-free areas, and spectra of Co atoms were acquired by positioning the tip over the center of each adatom protrusion. Spectra measured on different Co atoms on ML Pd look alike, suggesting that there is a preferential adsorption site, i.e., only one type of threefold hollow sites is occupied. Since the same Co atoms and also positions on Pd_nCo were measured at $B = +2$ T and $B = -2$ T, the electronic features related to differences in the local environment, such as different stacking and different lateral distances to the island edge, are the same for the spectra shown in Fig. 6(b). Therefore, the observed spectroscopic differences on the Co adatoms and the Pd layers are purely magnetic in origin.

Magnetic asymmetries of the spin-polarized spectra were calculated using Eq. (1) and are plotted in Fig. 6(c). We find that the Co adatoms on both ML and DL Pd show a similar energy-dependent asymmetry over the whole bias range studied from $U = -1$ V to $U = +1$ V (the same trend can be seen for the Pd layers as well). This means that the spin-polarized LDOS measured in vacuum above the Co adatoms (and Pd layers) does not change significantly with increasing Pd spacer thickness from ML to DL. This observation indicates the same nature of magnetic properties of Co adatoms on ML and DL Pd.

2. *Theory and discussion*

To investigate the coupling of Co adsorbed on the polarized Pd layers on Co/Ir(111) we first consider fully closed Co layers on Pd_nCo/Ir(111) ($n = 1$–3). Our DFT calculations show that, regardless of the stacking, Co adlayers on ML, DL, and also three layers of Pd carry a magnetic moment of about 2.04 μ_B/atom, with an induced magnetic moment of Pd of 0.29–0.35 μ_B/atom, except for the middle of the Pd trilayer (see Fig. 7). The values are in good qualitative agreement with results in Ref. 28, where it was reported that the magnetic moments of Co layers are 2.08–2.18 μ_B/atom with induced magnetic moments of ML and DL Pd of 0.19–0.30 μ_B/atom. However, we found that the calculated values of the exchange energy E_{exc} between the top Co layer and the Co/Ir(111) layer strongly decrease (see Fig. 7). While the Co layers align ferromagnetically for both the ML as well as the DL Pd spacer, the size of the coupling is reduced by a factor of three with increasing Pd thickness; the coupling across the Pd trilayer is almost zero (see Fig. 7).

This finding of a reduced coupling having the same sign for ML and DL spacer is in contrast to the calculation in Ref. 3 for single Co atoms coupled through a Cu spacer to Co/Cu(111). They find that the coupling is oscillatory (changing sign) and mediated by conduction electrons of the spacer. The electrons scattered from the Co layer form spin-polarized interference patterns inside the spacer due to quantum confinement.[3,29] These patterns vary with the spacer thickness, which causes the coupling of adatoms to oscillate between FM and AFM coupling, i.e., from parallel alignment for a ML Cu spacer to antialignment for a DL Cu spacer. The crucial difference to our system is that the Cu spacer was considered to be nonmagnetic, while the Pd layers in the present study carry an induced magnetic moment. This has a dramatic effect on the spacer thickness dependence of the interlayer exchange coupling, as also shown in the previous study of a Fe/Pd_n/Fe layer system[30]: by varying the Pd spacer thickness they found that the oscillatory behavior of the coupling between the magnetic layers is superimposed on the exponentially decreasing FM contribution. In their study this leads to an overcompensation

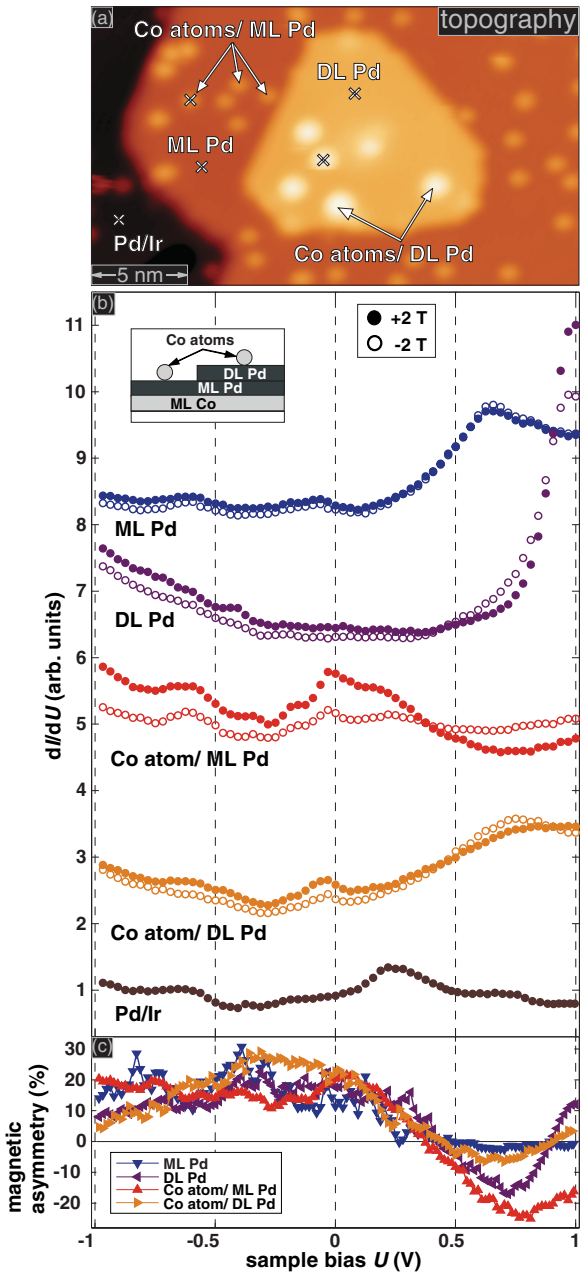

FIG. 6. (Color online) SP-STM measurements of Co atoms on DL Pd as well as on ML Pd on Co/Ir(111): (a) Constant-current image measured at $B = +2$ T. (b) Spin-polarized dI/dU spectra ($U_{\mathrm{stab}} = +1$ V, $I_{\mathrm{stab}} = 1$ nA, $U_{\mathrm{mod}} = 30$ mV) measured at $B = \pm 2$ T at locations marked by crosses in (a). Each spectrum is an average of five single spectra. All spectra except that of Pd/Ir are vertically shifted by multiples of 2 arb. units for clarity. (c) Magnetic asymmetries calculated for the spin-resolved spectra.

of the AFM part of the oscillatory coupling for $n \leqslant 12$ ML of Pd spacer. Furthermore, the FM coupling of Co layers through ML and DL Pd was reported in the theoretical study in Ref. 28 supported by experimental results in Refs. 31 and 32.

Coming back to the system studied here we suggest that the FM coupling via both the ML and DL Pd can be attributed to an additional FM contribution to the coupling, which is due to the induced magnetic moments of the Pd spacer. To obtain

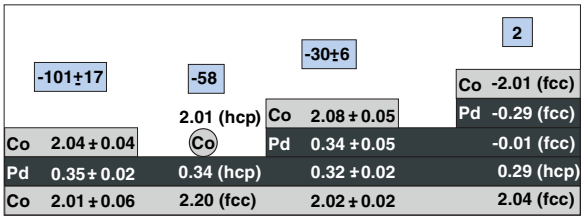

FIG. 7. (Color online) Results of DFT calculations of layers of $CoPd_nCo/Ir(111)$ $n = 1$–3 and a (2×2) Co atom superstructure on PdCo/Ir(111): Values inside of each layer and over the atom are magnetic moments (μ_B/atom) averaged over different stacking combinations with standard deviation, or calculated for the most stable stackings (noted). Numbers in blue boxes are exchange energies (meV/atom) of Co overlayers or of a single Co atom coupled to an underlying Co layer across a Pd spacer.

more realistic values for the coupling we also considered a (2×2) superstructure of Co atoms on a PdCo/Ir(111) system (cf. Fig. 7). We find an increase of the magnetic moment of the Co/Ir(111) layer, but the moments of the Pd spacer and the top Co atoms are similar to the previously discussed layered systems. Again, the coupling between the Co structures is FM, but compared to the layered system it is reduced from about -100 to -58 meV/top Co atom. If we consider the trend found for the closed Co layers, i.e., a decrease of the coupling via ML to DL Pd by a factor of three, we estimate a coupling of single Co atoms to the Co/Ir(111) through a Pd DL on the order of -17 meV/top Co atom. This also suggests a strong FM coupling, in line with the similar behavior of magnetic asymmetries of Co atoms on ML and DL Pd obtained in our SP-STM experiments (see Sec. III B1).

IV. SUMMARY

We have examined the system of Pd adlayers on Co/Ir(111) and Co atoms adsorbed on top. While for Co on Ir(111) only one type of stacking is present, we observe two stackings of ML Pd on Co islands, in agreement with our DFT calculations. The measured spin-polarized dI/dU contrast on ML and DL Pd indicates that Pd-capped Co islands are single domain ferromagnetic with the easy magnetization axis normal to the surface. Spin contrast is also achieved on Co adatoms on ML and DL Pd. We find that magnetic asymmetries of the measured spin-polarized spectra of Co atoms on Pd ML and DL show a similar energy-dependent behavior over the whole bias range studied from $U = -1$ V to $U = +1$ V. Based on our DFT calculations, we find that Pd atoms carry an induced magnetic moment on the order of 0.2–0.4 μ_B/atom. Calculations also predict that the coupling between Co structures through ML and DL Pd is ferromagnetic, which is supported by the spin-resolved STM measurements. Theory finds a reduction by a factor of three from a ML to DL Pd spacer, while it is close to zero for a spacer of three Pd layers.

ACKNOWLEDGMENTS

Financial support from the Deutsche Forschungsgemeinschaft via SFB 668-A1, -A8, from the ERC Advanced Grant FURORE, and from the Hamburg Cluster of Excellence NANOSPINTRONICS is gratefully acknowledged.

*ldzemian@physnet.uni-hamburg.de

[1]F. Meier, L. Zhou, J. Wiebe, and R. Wiesendanger, Science **320**, 82 (2008).
[2]A. A. Khajetoorians, J. Wiebe, B. Chilian, and R. Wiesendanger, Science **332**, 1062 (2011).
[3]O. O. Brovko, P. A. Ignatiev, V. S. Stepanyuk, and P. Bruno, Phys. Rev. Lett. **101**, 036809 (2008).
[4]Y.-S. Fu, Q.-K. Xue, and R. Wiesendanger, Phys. Rev. Lett. **108**, 087203 (2012).
[5]J. Prokop, A. Kukunin, and H. J. Elmers, Phys. Rev. B **75**, 144423 (2007).
[6]L. V. Dzemiantsova, M. Karolak, F. Lofink, A. Kubetzka, B. Sachs, K. von Bergmann, S. Hankemeier, T. O. Wehling, R. Frömter, H. P. Oepen, A. I. Lichtenstein, and R. Wiesendanger, Phys. Rev. B **84**, 205431 (2011).
[7]R. Decker, J. Brede, N. Atodiresei, V. Caciuc, S. Blügel, and R. Wiesendanger, submitted (2012).
[8]L. Berbil-Bautista, S. Krause, T. Hänke, M. Bode, and R. Wiesendanger, Surf. Sci. **600**, L20 (2006).
[9]J.-F. Jia, S.-C. Li, Y.-F. Zhang, and Q.-K. Xue, J. Phys. Soc. Jpn. **76**, 082001 (2007).
[10]M. Getzlaff, *Fundamentals of Magnetism* (Springer, Berlin, 2008).
[11]A. Enders, R. Skomski, and J. Honolka, J. Phys.: Condens. Matter **22**, 433001 (2010).
[12]R. Wiesendanger, Rev. Mod. Phys. **81**, 1495 (2009).
[13]O. Pietzsch, A. Kubetzka, D. Haude, M. Bode, and R. Wiesendanger, Rev. Sci. Instrum. **71**, 424 (2000).
[14]J. Tersoff and D. R. Hamann, Phys. Rev. Lett. **50**, 1998 (1983).
[15]J. Li, W.-D. Schneider, and R. Berndt, Phys. Rev. B **56**, 7656 (1997).
[16]J. E. Bickel, F. Meier, J. Brede, A. Kubetzka, K. von Bergmann, and R. Wiesendanger, Phys. Rev. B **84**, 054454 (2011).
[17]http://www.flapw.de.
[18]The spin-averaged spectra were calculated by $dI/dU_i = (dI/dU_{i\uparrow} + dI/dU_{i\downarrow})/2$, where i is A or B, indicating different stackings of Pd.
[19]H. Brune, C. Romainczyk, H. Röder, and K. Kern, Nature (London) **369**, 469 (1994).
[20]H. Brune, H. Röder, C. Romainczyk, C. Boragno, and K. Kern, Appl. Phys. A **60**, 167 (1995).
[21]M. Hohage, M. Bott, M. Morgenstern, Z. Zhang, T. Michely, and G. Comsa, Phys. Rev. Lett. **76**, 2366 (1996).
[22]T. Michely, M. Hohage, M. Bott, and G. Comsa, Phys. Rev. Lett. **70**, 3943 (1993).
[23]R. Q. Hwang, J. Schröder, C. Günther, and R. J. Behm, Phys. Rev. Lett. **67**, 3279 (1991).
[24]W. U. Fengmin, J. Zhang, G. Bian, and Z. Wu, Surf. Sci. **6**, 61 (2001).
[25] We also checked for magnetism the transition area where Pd is attached to Co rims. However, no spin-related contrast was observed at $T = 8$ K and $B = +1$ T.
[26]S. Blügel, B. Drittler, R. Zeller, and P. H. Dederichs, Appl. Phys. A **49**, 547 (1989).
[27] The line section across the domain wall in Fig. 5(b) was fitted by a standard wall profile for a 180° Bloch wall, $\tanh[(x)/(w/2)]$, where x is the lateral distance and w is the domain wall width.
[28]K. Miura, H. Kimura, S. Imanaga, and Y. Hayafuji, J. Appl. Phys. **72**, 4826 (1992).
[29]P. Bruno, Phys. Rev. B **52**, 411 (1995).
[30]Y. Takahashi, J. Appl. Phys. **85**, 5744 (1999).
[31]H. J. G. Draaisma, W. J. M. de Jonge, and F. J. A. den Broeder, J. Magn. Magn. Mater. **66**, 351 (1987).
[32]J. V. Harzer, B. Hillebrands, R. L. Stamps, G. Güntherdt, C. D. England, and M. Falco, J. Appl. Phys. **62**, 2448 (1991).